

Article

Prediction of Thermal Energy Demand Using Fuzzy-Based Models Synthesized with Metaheuristic Algorithms

Hamzah Ali Alkhazaleh ¹, Navid Nahi ², Mohammad Hossein Hashemian ³, Zohreh Nazem ⁴,
Wameed Deyah Shamsi ⁵ and Moncef L. Nehdi ^{6,*}

- ¹ College of Engineering and IT, University of Dubai, Academic City, Dubai 14143, United Arab Emirates
² Department of Architecture, Islamic Azad University, Tehran Science and Research Branch (East Azerbaijan), Tehran 14778-93855, Iran
³ Department of Architecture, Tehran University, Kish Campus, Kish 13114-16846, Iran
⁴ Department of Architecture and Urban Design, Islamic Azad University Qazvin Branch, Qazvin 34185-1416, Iran
⁵ Information Technology Unit, Al-Mustaqbal University College, Babylon 51001, Iraq
⁶ Department of Civil Engineering, McMaster University, Hamilton, ON L8S 4L8, Canada
* Correspondence: nehdim@mcmster.ca

Abstract: Increasing consumption of energy calls for proper approximation of demand towards a sustainable and cost-effective development. In this work, novel hybrid methodologies aim to predict the annual thermal energy demand (ATED) by analyzing the characteristics of the building, such as transmission coefficients of the elements, glazing, and air-change conditions. For this objective, an adaptive neuro-fuzzy-inference system (ANFIS) was optimized with equilibrium optimization (EO) and Harris hawks optimization (HHO) to provide a globally optimum training. Moreover, these algorithms were compared to two benchmark techniques, namely grey wolf optimizer (GWO) and slap swarm algorithm (SSA). The performance of the designed hybrids was evaluated using different accuracy indicators, and based on the results, ANFIS-EO and ANFIS-HHO (with respective RMSEs equal to 6.43 and 6.90 kWh·m⁻²·year⁻¹ versus 9.01 kWh·m⁻²·year⁻¹ for ANFIS-GWO and 11.80 kWh·m⁻²·year⁻¹ for ANFIS-SSA) presented the most accurate analysis of the ATED. Hence, these models are recommended for practical usages, i.e., the early estimations of ATED, leading to a more efficient design of buildings.

Keywords: sustainability; building energy; thermal energy demand; ANFIS; Harris hawks optimization



check for updates

Citation: Alkhazaleh, H.A.; Nahi, N.; Hashemian, M.H.; Nazem, Z.; Shamsi, W.D.; Nehdi, M.L. Prediction of Thermal Energy Demand Using Fuzzy-Based Models Synthesized with Metaheuristic Algorithms.

Sustainability **2022**, *14*, 14385.

<https://doi.org/10.3390/su142114385>

Academic Editor: Cinzia Buratti

Received: 28 September 2022

Accepted: 26 October 2022

Published: 3 November 2022

Publisher's Note: MDPI stays neutral with regard to jurisdictional claims in published maps and institutional affiliations.



Copyright: © 2022 by the authors. Licensee MDPI, Basel, Switzerland. This article is an open access article distributed under the terms and conditions of the Creative Commons Attribution (CC BY) license (<https://creativecommons.org/licenses/by/4.0/>).

1. Introduction

Enhancements in living standards has necessitated a significant increase in energy consumption of buildings [1]. A large portion of energy is consumed for providing suitable space cooling and heating. For instance, this contribution has been reported around 48% in the U.S. and 65% in the European Union [2,3]. Therefore, preparing an efficient estimation of heating load (HL) and cooling load (CL) based on the characteristics of the building is a crucial task towards energy conservation and environmental protection [4].

From a more general perspective, the world of science and especially engineering domains have experienced significant advances in different fields [5,6]. A wide variety of methodologies and apparatuses have been developed with the aim of facilitating existing problems [7,8]. More particularly, for energy issues, many of these inventions have been tried by energy experts to increase the efficiency of energy systems (e.g., recharging and consumption systems [9,10]). Another objective has been achieving a reliable and inexpensive estimation of energy demand in buildings with various usages (e.g., office, residential, school, etc.) [11,12]. An increasingly popular approach in dealing with energy performance simulations is machine learning. Machine learning models, owing to their potential in understanding and reproducing complicated non-linear patterns, have been

used for mapping the relationship between various engineering-based parameters and the corresponding effective factors [13,14]. As for energy-related analysis, many scholars have successfully applied intelligent models such as artificial neural networks (ANNs) [15], regression-oriented approaches [16], support vector machine (SVM) [17], etc. Provided with a valid dataset, these models aim to learn the pattern of energy parameters affected by multiple changes in the influential parameters.

The adaptive neuro-fuzzy inference system (ANFIS) is known as one of the most capable machine learning tool widely used for energy prediction works [18]. Bilgili et al. [19] demonstrated the suitability of ANFIS for estimating renewable electricity generation. Baetens et al. [20] used this model for evaluating the thermal performance of cooling load systems. Gao et al. [21] could accurately analyze the performance of integrated photovoltaic-thermal system. This model attained above 99% correlation between its outputs and real-world values. Another successful application of ANFIS was reported by Ekici and Aksoy [22] for building energy load-forecasting area. Alam and Ali [23] employed ANFIS with a subtractive clustering method for estimation of building energy consumption. Based on the findings from comparison with ANN, ANFIS can present more accurate result. Further comparative studies among diverse machine learning can be found in the literature [24,25].

In many cases, coupling a predictive model with other existing techniques results in improving the efficiency of the model. Therefore, numerous studies have been dedicated to combining machine learning tools with sophisticated techniques. For example, Nilashi et al. [26] used a combination of ANFIS with expectation maximization and principal component analysis to appraise the CL and HL. The results professed great promise for the applied model with reference to mean absolute errors (MAEs) of 0.52 and 0.16, respectively.

One of the most beneficial ideas for combining with machine learning methods is the use of metaheuristic algorithms. These algorithms try to improve their performance by overcoming computational deficiencies [27–29]. Several applications of these algorithms can be mentioned for optimizing regular predictors for energy-prediction problems. Kardani et al. [30] optimized the ANFIS using biogeography-based optimization (BBO) and improved particle swarm optimization (IPSO) for predicting HL and CL in residential building. Achieving more than 83% concordance between the real and modeled values, both hybrid models were introduced as promising predictors for this purpose. Alduailij, Petri, Rana, Alduailij, and Aldawood [15] proposed a combination of SVM and imperialistic competitive algorithm (ICA) for predicting 24 h ahead of heat demand. The proposed methodology could achieve more promising results compared to typical SVM and improved ANN models. Almutairi et al. [31] assessed four ANNs optimized with firefly algorithm (FA), shuffled complex evolution (SCE), optics-inspired optimization (OIO), and teaching–learning-based optimization (TLBO) and concluded that TLBO-ANN, with above 96% correlation, yields the most reliable results. Further research efforts that have been devoted to conduct a comparison among the metaheuristic algorithms can be found in earlier studies [32,33].

An eminent conclusion from the above literature is that utilizing metaheuristic algorithms in combination with regular predictive models leads to novel methodologies that perform better than single versions. According to similar studies, the reason behind this improvement lies in the capability of metaheuristic optimizers in remedying the computational deficiencies associated with single regular models [34,35]. More particularly for the ANFIS, however, training this model is susceptible to drawbacks such as local minima and dimension danger, but the incorporation of metaheuristic algorithms can overcome these issues through tuning the parameters of membership function (MFPs) [36,37]. Hence, in order for ANFIS to achieve a reliable solution for complicated problems such as energy-demand analysis, it is essential to be hybridized with appropriate optimization algorithms.

On the other hand, conventional types of metaheuristic algorithms have been sufficiently investigated in different sectors. For example, PSO [38,39] and the genetic algo-

rithm (GA) [40] are among the most popular optimizers served in optimizing ANFIS for energy-demand predictions. Based on many recent research efforts, the new generation of metaheuristic algorithms is introducing potential optimizers whose competency needs to be evaluated and professed. Hereupon, this study aims to bridge the gap between the latest artificial intelligence advances and convenient energy-demand analysis. In this sense, two capable metaheuristic algorithms, namely equilibrium optimization (EO) and Harris hawks optimization (HHO), are employed in combination with ANFIS for predicting the annual thermal energy demand (ATED). The EO and HHO are well-tried algorithms for optimization purposes in energy-related domains [41,42]. For instance, Zayed et al. [43] declared the high capacity of EO-ANFIS for analyzing the energetic performance of a solar dish collector. In addition, two well-known optimization techniques, namely grey wolf optimizer (GWO) and slap swarm algorithm (SSA), are also employed as benchmarks to comparatively validate the performance of the HHO and EO.

In the following, the paper is organized as follows: the used data and employed algorithms are introduced in Section 2; the results (i.e., performance of the models) are presented, compared, and discussed in Section 3; and the main findings are highlighted in the conclusion, Section 4.

2. Materials and Methods

2.1. Used Dataset

To be able to predict the ATED, the hybrid models proposed in this work must analyze a set of historical samples. The quality and validity of this data are important parameters to be considered [44,45]. Taken from a previous study by Chegari et al. [46], the data of this study are composed of twelve parameters comprising (a) eleven input parameters, namely U_M : transmission coefficient of the external walls ($W \cdot m^{-2} \cdot K^{-1}$), U_T : transmission coefficient of the roof ($W \cdot m^{-2} \cdot K^{-1}$), U_P : transmission coefficient of the floor ($W \cdot m^{-2} \cdot K^{-1}$), α_M : solar radiation absorption coefficient of the exterior walls, α_T : solar radiation absorption coefficient of the roof, P_t : linear coefficient of thermal bridges ($W \cdot m^{-1} \cdot K^{-1}$), ACH: air change rate ($v \cdot h^{-1}$), Scw-N: shading coefficient of north-facing windows, Scw-S: shading coefficient of south-facing windows, Scw-E: shading coefficient of east-facing windows, and Glz: glazing; and (b) a target parameter called ATED ($kWh \cdot m^{-2} \cdot year^{-1}$). Noting that, ATED here is considered as a combination of total heat demand for cooling (Q_c) and heating (Q_h) with respect to total surface of conditioned zones (A_c), as expressed in the below equation:

$$ATED = \frac{(Q_c + Q_h)}{A_c} \quad (1)$$

Figure 1 shows the scatter charts illustrating the relationship between the ATED and each input parameter. As is observed, the ATED has a similar trend with respect to all inputs except Glz. All inputs are directly proportional to the ATED, while the general trend of Glz falls with the increase of ATED.

The used dataset consists of 35 records. To attain the objective of the study, two sets of data are required: one with 80% of records forming the training set and the other with 20% of records forming the testing set. It is a well-established rule that for a prediction task, the model should be first trained. In this regard, a predictive model analyzes the interrelated relationship between the target parameter (here, ATED) and influential parameters (here, U_M , U_T , U_P , α_M , α_T , P_t , ACH, Scw-N, Scw-S, Scw-E, and Glz). Once the training is accomplished, its quality is tested by considering testing data. In both stages, the prediction products of the model are compared to real values, and the accuracy is calculated using appropriate indicators.

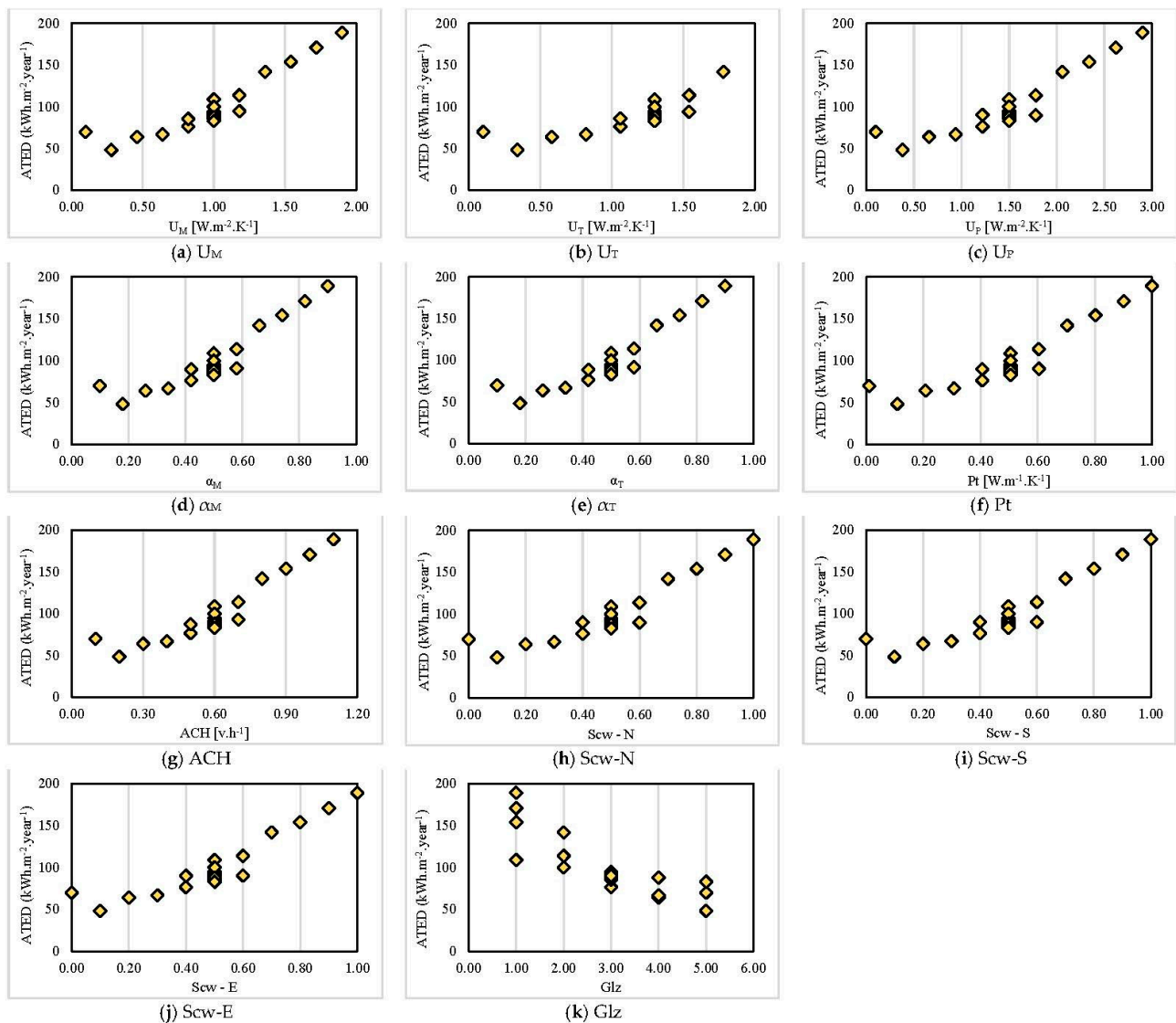


Figure 1. Scatter charts showing the relationship between the ATED and (a) U_M . (b) U_T . (c) U_F . (d) α_M . (e) α_T . (f) Pt . (g) ACH . (h) $Scw-N$. (i) $Scw-S$. (j) $Scw-E$. (k) Glz .

2.2. Employed Algorithms

2.2.1. ANFIS

ANFIS is a leading model in prediction tasks. This model was developed by Jang [47] in 1993, and so far, it has served strongly in diverse, complex simulations, especially in energy sectors [38]. As the name of this model indicates, two major parts that form the ANFIS are the neural part that is taken from the self-learning ability of ANNs and fuzzy part that represents the expression function of the fuzzy technique. The simulation using ANFIS is started with creating if-then rules corresponding to MFs. By tweaking these rules and MFs, the model shapes the relationship between target and input factors. Figure 2 shows the five-layered topology of the ANFIS.

Layer 1 contains the MFs used for the fuzzification applied to the inputs. Layer 2 contains multiplier rules and releases a strength from each node. Layer 3 deals with the normalization process applied to the calculated strengths. Next, the output MFs is presented in Layer 4 by its adaptive nodes. The global response is finally released by the node in Layer 5, which sums up the previous outputs [48].

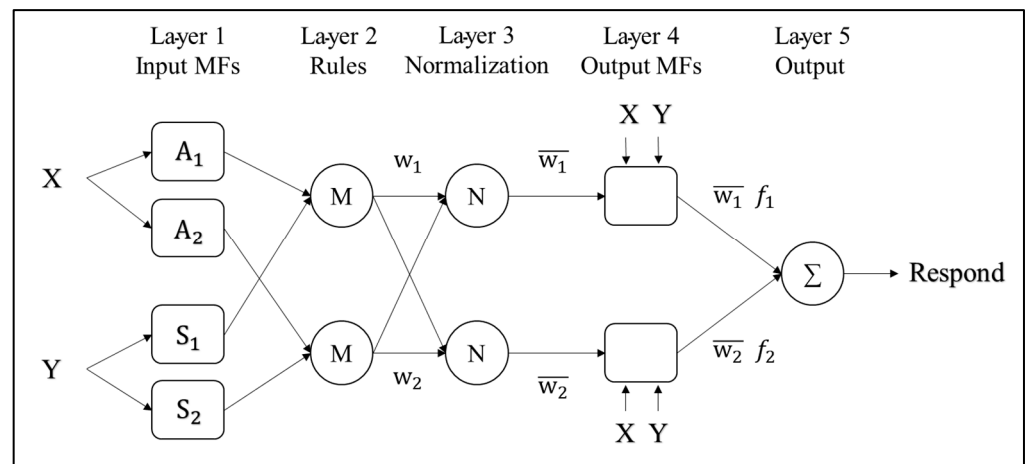


Figure 2. General topology of the ANFIS.

2.2.2. Metaheuristic Algorithms

Four metaheuristic algorithms that are synthesized with ANFIS are EO, GWO, HHO, and SSA. These algorithms are known as population-based techniques, meaning that a pre-defined number of individuals search the space of the problem to discover the optimum solution. In this process, each algorithm follows a specific strategy for updating the position of the population within search space. These techniques are explained in the following.

The EO was designed by Faramarzi et al. [49]. In this algorithm, a control volume is simulated, wherein the equation of mass balance expresses the concentration of components. An equilibrium pool is formed by citing the concentration of three outstanding particles along with an average of them, and updating these concentrations represents the optimization process in the EO [50].

Unlike the EO, which is a physics-inspired technique, the idea of GWO, HHO, and SSA is taken from the social behavior of grey wolves, Harris hawks, and salps. These algorithms were, respectively, proposed by Mirjalili et al. [51], Heidari et al. [52], and Mirjalili et al. [53]. In the GWO, the herd is divided into four classes, namely alpha, beta, delta, and omega. As is known, alpha and omega wolves are characterized with the highest power. The first three classes are responsible for seeking prey, while the omega class plays the role of assistant. The distance from the prey is considered as the fitness of the solution, and the algorithm updates the wolves' position to better approach the prey. The same happens in the HHO to track and hunt. In general terms, the steps in which the target is sought and hunted are called exploration and exploitation, respectively. Likewise, for the SSA, the chain of salps is composed of a leader, i.e., the most powerful individual, that is followed by others toward attaining a food source that is updated with more promising ones for fulfilling the optimization.

Since the mathematical configuration of these algorithms is quite computer-science-oriented and is out of the scope of this work, the readers may refer to the appropriate literature (EO [54,55], GWO [56,57], HHO [58,59], and SSA [60,61]) for more detailed information and latest updates regarding these algorithms.

3. Results and Discussion

3.1. Accuracy Equations

To validate and compare the prediction robustness of the suggested ANFIS-HHO model, four accuracy indicators were applied to the results to express the error of prediction (i.e., the difference between the real and estimated ATEDs) as well as their concordance (i.e., the correlation between the real and estimated ATEDs). The index that gives the correlation is Pearson correlation index (R_p) introduced in Equation (2), wherein $ATED_{i_{estimated}}$ and $ATED_{i_{real}}$ represent the estimated and real values with averages given by \overline{ATED} . Moreover, SZ signifies the size of dataset. Similarly, the MAE and RMSE calculate the error in the

absolute format based on Equations (3) and (4), while Equation (5) releases a relative form of error called mean absolute percentage error (MAPE) [62,63].

$$R_p = \frac{\sum_{i=1}^{SZ} (ATED_{i_{estimated}} - \overline{ATED}_{estimated})(ATED_{i_{real}} - \overline{ATED}_{real})}{\sqrt{\sum_{i=1}^{SZ} (ATED_{i_{estimated}} - \overline{ATED}_{estimated})^2} \sqrt{\sum_{i=1}^{SZ} (ATED_{i_{real}} - \overline{ATED}_{real})^2}} \quad (2)$$

$$MAE = \frac{1}{SZ} \sum_{i=1}^{SZ} |ATED_{i_{real}} - ATED_{i_{estimated}}|, \quad (3)$$

$$RMSE = \sqrt{\frac{1}{SZ} \sum_{i=1}^{SZ} [(ATED_{i_{real}} - ATED_{i_{estimated}})]^2}, \quad (4)$$

$$MAPE = \frac{1}{SZ} \sum_{i=1}^{SZ} \left| \frac{ATED_{i_{real}} - ATED_{i_{estimated}}}{ATED_{i_{real}}} \right| \times 100, \quad (5)$$

Needless to say, the model with a lower RMSE, MAE, and MAPE and higher R_p represents more consistent results. Thus, based on the combination of these indices, the ranking of models can be developed.

3.2. Hybridization, Optimization, and Network Selection

The name ANFIS-HHO represents a hybrid methodology composed of ANFIS predictor and HHO optimization algorithm. It was earlier elucidated that the HHO aims to optimize the MFPs existing in the ANFIS [64]. Constructing the hybrid model should be performed by means of some middle measures (i.e., equations). On the other hand, optimization by metaheuristic algorithms is done inchmeal over a certain number of iterations [65,66]. Thus, an evaluation criterion is required to monitor the results of each iteration. The RMSE indicator is defined as the cost function (i.e., objective function) to show the accuracy of the optimized ANFIS. It will be shown that the assigned metaheuristic algorithm is able to reduce the RMSE step by step, which indicates improving the training of ANFIS [67].

There are two user-determined parameters, namely the number of iterations and population size for the metaheuristic optimizers. Based on earlier studies and investigating the behavior of algorithms, the EO, GWO, HHO, and SSA are executed with 1000 iterations in this work [68,69]. Population size, in most metaheuristic algorithms developed so far, denotes the number of active individuals that look for the optimum solution. Hence, it can broadly affect the performance of the algorithms. Trial and error is a well-accepted approach for finding a suitable population size for each application of metaheuristic algorithms [35]. Accordingly, for this study, trying five common populations (i.e., 100, 200, 300, 400, and 500) resulted in widely different optimization results for the intended algorithms. The results are shown in Table 1.

Table 1. RMSE results for five different population sizes.

Population Size	ANFIS-EO		ANFIS-GWO		ANFIS-HHO		ANFIS-SSA	
	Train	Test	Train	Test	Train	Test	Train	Test
100	5.672	6.432	12.031	11.395	5.880	6.905	11.716	11.801
200	3.477	11.721	11.369	9.011	2.249	7.814	4.070	33.542
300	3.535	13.168	25.504	73.984	3.497	32.289	11.178	12.099
400	2.606	13.227	11.144	11.294	4.479	7.698	2.667	19.422
500	4.943	6.848	11.367	9.042	3.221	12.461	11.051	12.129
Min. RMSE	2.606	6.432	11.144	9.011	2.249	6.905	2.667	11.801

Based on Table 1, each model yielded the smallest RMSEs, i.e., the best accuracy, for different populations. The ANFIS-EO, ANFIS-GWO, ANFIS-HHO, and ANFIS-SSA with populations 400, 400, 200, and 400 gave the most accurate training, while the best testing results were obtained for populations 100, 200, 100, and 100, respectively. Therefore, the results of this models are presented and discussed in the following sections. Table 2 expresses the name of the models with reference to the selected population sizes.

Table 2. Nomenclature of the models based on population size.

Framework	Metaheuristic Optimizer	Population Size	Final Name	Phase
ANFIS	EO	400	ANFIS-400-EO	Train
ANFIS	EO	100	ANFIS-100-EO	Test
ANFIS	GWO	400	ANFIS-400-GWO	Train
ANFIS	GWO	200	ANFIS-200-GWO	Test
ANFIS	HHO	200	ANFIS-200-HHO	Train
ANFIS	HHO	100	ANFIS-100-HHO	Test
ANFIS	SSA	400	ANFIS-400-SSA	Train
ANFIS	SSA	100	ANFIS-100-SSA	Test

3.3. Accuracy Assessment

Once the models are determined, their performance is examined in this section. The results are generally presented for (a) the training phase that shows the quality of ATED pattern captured by each model and (b) the testing phase that shows the quality of ATED prediction for stranger buildings. Table 3 collects the results of both phases in terms of introduced accuracy indicators.

Table 3. Summarized accuracy assessment results.

Phase	Model	MAE	RMSE	R _p	MAPE
Train	ANFIS-400-EO	1.87	2.60	0.99	1.86
	ANFIS-400-GWO	7.63	11.14	0.90	8.17
	ANFIS-200-HHO	1.91	2.24	0.99	2.08
	ANFIS-400-SSA	1.90	2.66	0.99	1.89
Test	ANFIS-100-EO	6.20	6.43	0.99	7.23
	ANFIS-200-GWO	6.75	9.01	0.97	6.41
	ANFIS-100-HHO	5.74	6.90	0.99	7.35
	ANFIS-100-SSA	9.07	11.80	0.93	8.93

In terms of RMSE, the ANFIS-400-EO, ANFIS-400-GWO, ANFIS-200-HHO, and ANFIS-400-SSA achieved an error of 2.60, 11.14, 2.24, and 2.66, respectively, in the training phase. Likewise, the RMSE of ANFIS-100-EO, ANFIS-200-GWO, ANFIS-100-HHO, and ANFIS-100-SSA yielded 6.43, 9.01, 6.90, and 11.80 in the testing phase. As for the MAE, training values were 1.87, 7.63, 1.91, and 1.90, and testing values were 6.20, 6.75, 5.74, and 9.07.

Figure 3 shows graphical comparisons between the patterns of real and estimated ATEDs. As is seen, in both training and testing figures, the real pattern (i.e., target with red line) is nicely followed by the estimated pattern (i.e., output with blue line) by all four models. This consistency can also be deduced from the calculated MAPEs, which are 1.86, 8.17, 2.08, and 1.89% in the training phase and 7.23, 6.41, 7.35, and 8.93% in the testing phase.

Figure 4 illustrates above results in the form of correlation charts. According to these charts, the R_p of all models is above 90%, which indicates an excellent harmony between the reality and the prediction of models. It is observed that for all models, the points are favorably aggregated around the ideal line (i.e., $x = y$ dashed line). It means that the values on the x -axis (=target) are very close to the corresponding values on the y -axis (=output), and therefore, it indicates high accuracy of prediction. However, there are some

underestimations and overestimations evident in some charts. The next sections elaborate on the comparison between prediction accuracies.

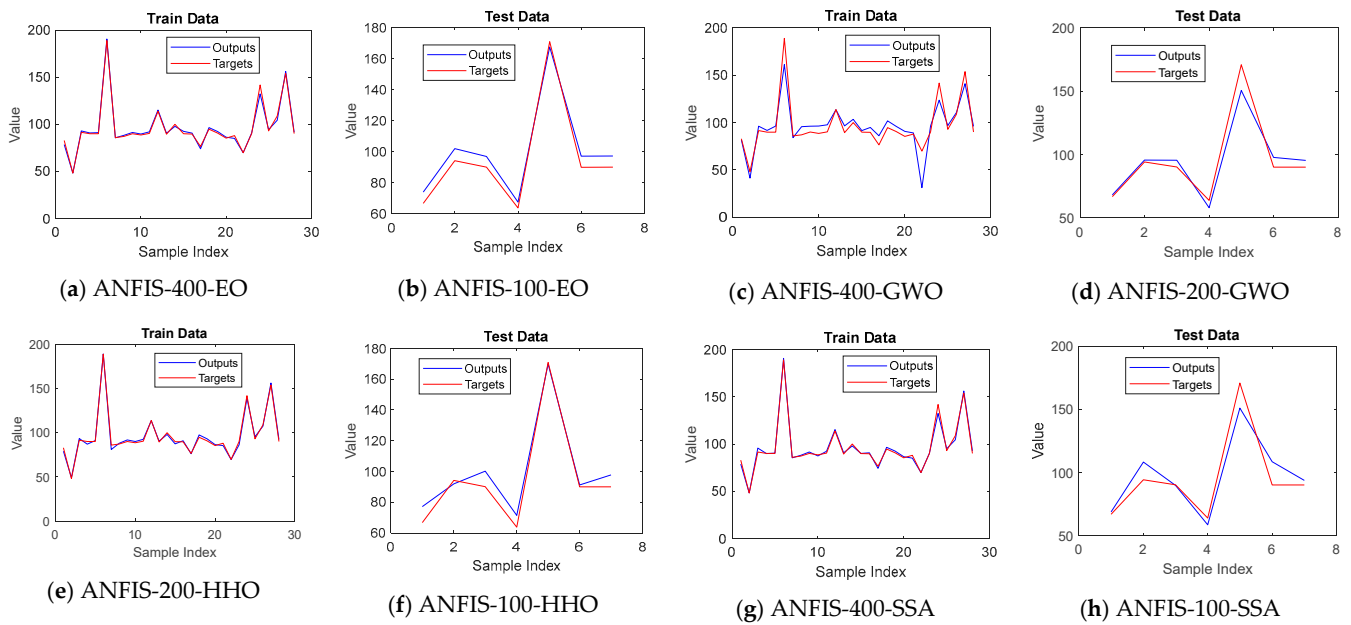


Figure 3. Pattern comparison in the training (a,c,e,g) and testing (b,d,f,h) phases.

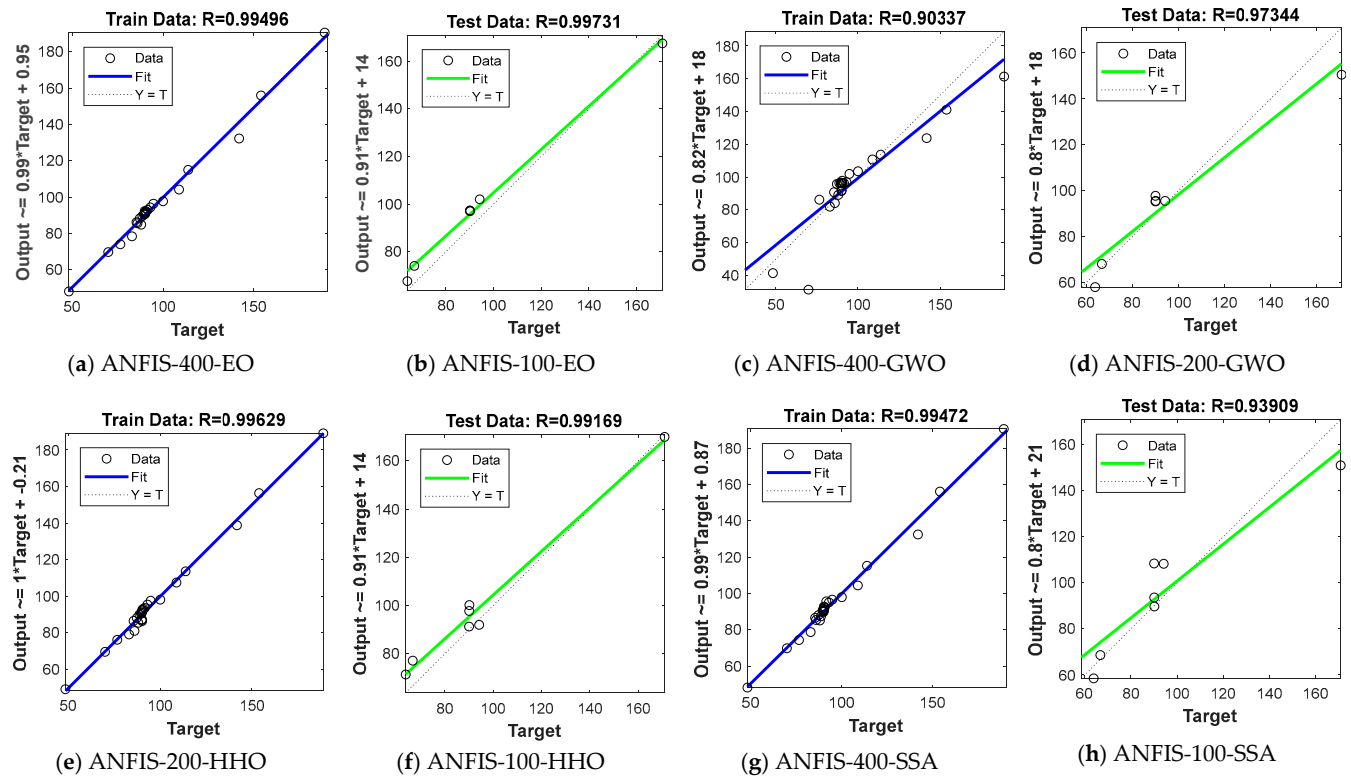


Figure 4. Correlation of results in the training (a,c,e,g) and testing (b,d,f,h) phases.

3.4. Ranking and Comparison

Although the performance of all hybrid models achieved a satisfying level of accuracy, there were some noticeable distinctions among them in the prediction of ATED values. Referring to the reported accuracy indicators (see Table 3), the EO-ANFIS was the best-trained hybrid based on the lowest MAE and MAPE obtained for this algorithm. Further, with a slight difference, EO-ANFIS attained the smallest RMSE after the HHO-ANFIS.

Hereupon, the EO can come up as the most reliable metaheuristic technique for training the ANFIS. Likewise, there is a close competition between the EO-ANFIS and HHO-ANFIS in the testing results. These models yielded the lowest RMSE and MAE, respectively. Moreover, despite the equal R_p values, the EO-ANFIS was the second-most-accurate model in terms of MAE, R_p , and MAPE.

Figure 5 shows Taylor diagrams for training and testing results for a more comprehensive comparison among the models. This diagram illustrates the correlation, standard deviation, and range of RMSE (i.e., RMSD in the graph) at the same time [70]. According to part (a) that corresponds to the training data, a significant distinction can be observed between the GWO and three other metaheuristic algorithms. It is also deduced that although the HHO slightly outperformed the SSA and EO with reference to correlation and RMSD values, the EO is characterized with a lower standard deviation. As for testing phase, part (b) demonstrates the absolute superiority of the EO owing to the tangible differences in the error and correlation simultaneously. After that, HHO gave the best prediction, followed by the GWO and SSA.

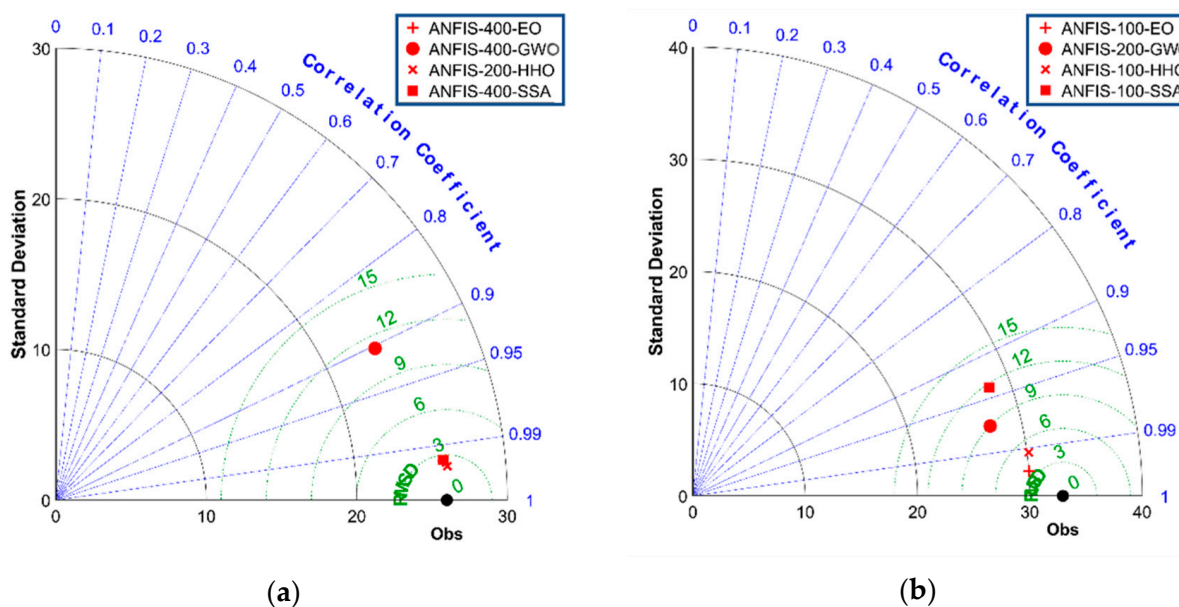


Figure 5. Taylor diagrams for comparison among the models in (a) training and (b) test phases.

Referring to the above assessment, a general ranking can be stated for the four used models. While both ANFIS-EO and ANFIS-HHO presented a strong robustness, the EO-ANFIS may deserve notation as the outstanding model of this study with respect to the cumulative effect of all accuracy indicators in both capturing and generalizing the ATED behavior. From the same reasoning, ANFIS-GWO and ANFIS-SSA had weaknesses in the training and testing phases, respectively. Therefore, they may not be preferred over the two other algorithms.

3.5. Additional Discussion

Prediction of thermal energy demand is essential for governments to formulate energy policies and adjust future strategies [71,72]. In this work, four sophisticated machine learning approaches were tested and validated for predicting the ATED by knowing eleven characteristics, namely U_M , U_T , U_P , α_M , α_T , P_t , ACH, Scw-N, Scw-S, Scw-E, and Glz. The developed methodologies are generalizable owing to the high accuracy acquired in testing phase.

In this sense, there could be important practical contribution of the offered models. They can predict the ATED for new, unseen building conditions. For instance, assuming an upcoming construction project, if the engineers have an approximation of the required

thermal load in hand, it enables them to design/select the appropriate heating, ventilation, and air conditioning (HVAC) systems. Since ATED is widely affected by the dimension and characteristics of the building, another application could be modification of the building plan, dimensions, etc., to attain an environmentally efficient design. To exemplify, in Figure 6, the variation of the ATED is depicted versus the variation of two input parameters. The general trend is clearly understandable, as the ATED rises with the increase of both U_M and P_t . In addition, observing the dashed lines in both figures shows that the used models (especially the ANFIS-HHO and ANFIS-EO) can nicely follow and predict this trend. The same can be created for other input parameters. Hence, performing such analysis on a large scale can be helpful to move towards sustainable energy consumption.

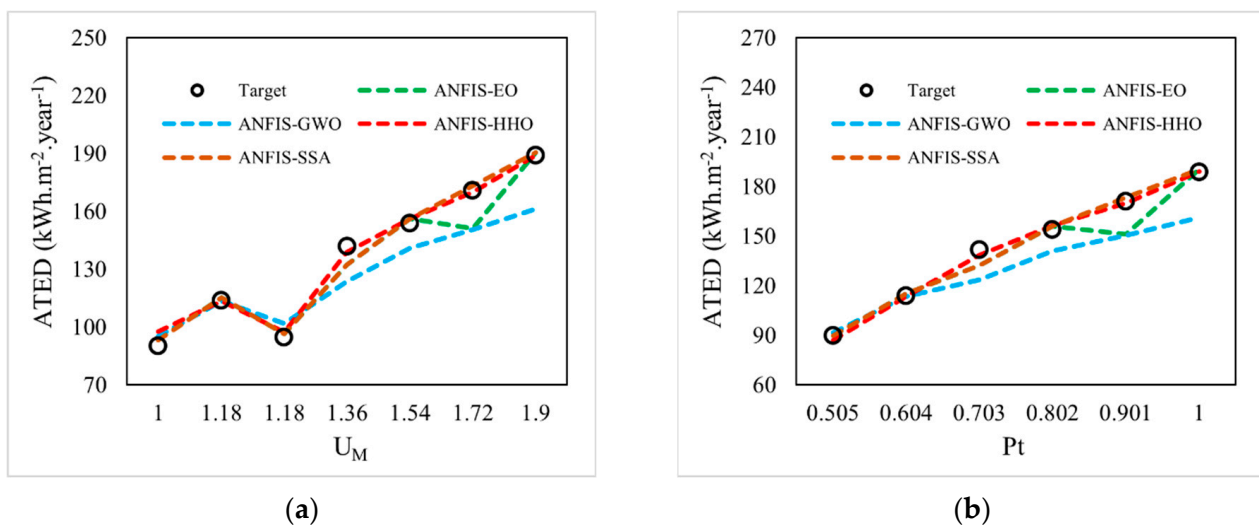


Figure 6. Trend of ATED with respect to the increase of (a) U_M and (b) P_t .

Although the performance of the models was generally acceptable, and desirable results were obtained, there are some points that can be considered as the limitations of this study. Moreover, some ideas can be suggested to address potential guidance for conducting future research.

Considering the optimization approach taken by each metaheuristic algorithm, Figure 7 depicts the path of RMSE reduction as explained in Section 3.2. As is seen, each algorithm has a specific reduction rate with respect to the number of iterations. The EO and HHO performed a major part of the task by around 700 iterations, during which the error is reduced step by step. This is while the GWO reached the optimum solution in approximately 100 iterations, and after that, its curve remained more or less fixed. However the SSA curve has two major steps that occurred in the beginning, and the second step starts before 500th iteration. We therefore raise the question of why the models are bounded to 1000 iterations. The reasons lie in (a) the behavior of the algorithms, in which, according to Figure 7, all models reach a steady level before 1000 iterations; (b) the general behavior of the algorithms that have yielded a reasonable solution with 1000 iterations in similar studies [73,74]; and (c) some limitations that exist regarding the time of calculations. As is known, an iterative process like this may take considerable time. Therefore, we should consider time as an important parameter in engineering works. For future works, utilizing powerful systems to implement more iterations can be recommended. However, it does not seem very likely to see a considerable improvement (see Figure 7).

This study only used ANFIS because it aimed at evaluating the effect of metaheuristic algorithms in equal conditions. While ANFIS is among the most outstanding prediction models, there are other capable tools such as ANN and SVM that may compete with ANFIS in this way. Hence, another worthwhile investigation subject is applying one metaheuristic algorithm to more basic models. As well as this, conducting comparative efforts among

more metaheuristic optimizers is recommended towards updating the solution as new algorithms are developed.

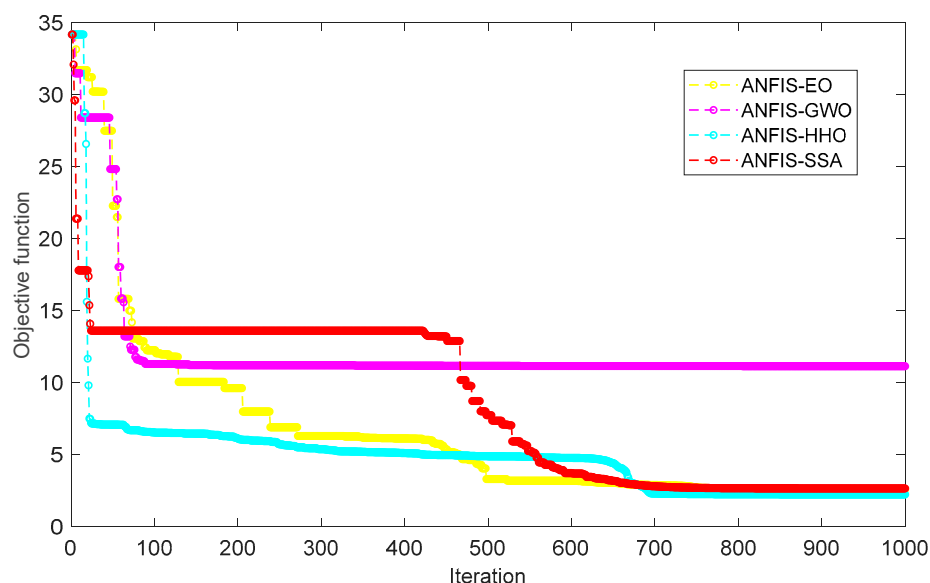


Figure 7. Path of optimizing ANFIS using metaheuristic techniques.

4. Conclusions

Having a good estimation of building energy demand is beneficial from different environmental and economical points of view. Therefore, developing reliable and cost-effective methodologies is of great importance in sustainable development of building energy systems. Although earlier literature has recommended the use of machine learning for this purpose, traditional approaches meet some deficiencies that can be remedied using new optimization algorithms. In this study, a fuzzy-based model called ANFIS was successfully optimized by the EO, GWO, HHO, and SSA metaheuristic algorithms to predict annual thermal energy demand. According to the results, the incorporation of these four algorithms can make ANFIS an accurate tool for understanding the behavior of ATED based on changes in the characteristics of the building and, subsequently, predicting the pattern for new circumstances. In detail,

- With correlation values > 90% and relative errors < 9%, all models achieved a satisfying accuracy in predicting the ATED.
- The performance of the ANFIS-EO and ANFIS-HHO were characterized with the smallest error and largest concordance of the results. The RMSE of 6.43 and 6.90 kWh·m⁻²·year⁻¹ were obtained for the ANFIS-EO and ANFIS-HHO versus 9.01 and 11.80 kWh·m⁻²·year⁻¹ for ANFIS-GWO and ANFIS-SSA, respectively.
- Referring to these outcomes, ANFIS-EO and ANFIS-HHO can be practical evaluators for tuning the performance of ongoing energy systems as well as designing appropriate systems for renovation and construction projects.
- Last but not least, the proposed informational model can offer a data-driven predictive tool with superior accuracy to enhance predictions and guide policy making for energy-saving policies towards enhanced sustainability of the built environment.

Author Contributions: Conceptualization and methodology, H.A.A. and M.H.H.; software, validation, and writing—original draft preparation, N.N. and H.A.A.; writing—review and editing, visualization, and project administration, Z.N., W.D.S. and H.A.A.; project administration and funding acquisition, M.L.N. All authors have read and agreed to the published version of the manuscript.

Funding: This research received no funding.

Conflicts of Interest: The authors declare no conflict of interest.

References

1. Gao, W.; Alsarraf, J.; Moayedi, H.; Shahsavari, A.; Nguyen, H. Comprehensive preference learning and feature validity for designing energy-efficient residential buildings using machine learning paradigms. *Appl. Soft Comput.* **2019**, *84*, 105748. [CrossRef]
2. Meir, A. Heating and cooling no longer majority of US home energy use. *Lead Househ. Prod.* **2013**, *8*. Available online: <http://www.homeenergy.org/show/article/magazine/130/id/1862> (accessed on 27 September 2022).
3. Eurostat. *Energy Consumption in Households*; Office for Official Publications of the European Communities: Luxembourg, 1993.
4. Li, X.; Yao, R. A machine-learning-based approach to predict residential annual space heating and cooling loads considering occupant behaviour. *Energy* **2020**, *212*, 118676. [CrossRef]
5. Wu, P.; Liu, A.; Fu, J.; Ye, X.; Zhao, Y. Autonomous surface crack identification of concrete structures based on an improved one-stage object detection algorithm. *Eng. Struct.* **2022**, *272*, 114962. [CrossRef]
6. Zhao, Y.; Hu, H.; Bai, L.; Tang, M.; Chen, H.; Su, D. Fragility analyses of bridge structures using the logarithmic piecewise function-based probabilistic seismic demand model. *Sustainability* **2021**, *13*, 7814. [CrossRef]
7. Zhao, Y.; Joseph, A.J.J.M.; Zhang, Z.; Ma, C.; Gul, D.; Schellenberg, A.; Hu, N. Deterministic snap-through buckling and energy trapping in axially-loaded notched strips for compliant building blocks. *Smart Mater. Struct.* **2020**, *29*, 02LT03. [CrossRef]
8. Yan, B.; Ma, C.; Zhao, Y.; Hu, N.; Guo, L. Geometrically Enabled Soft Electroactuators via Laser Cutting. *Adv. Eng. Mater.* **2019**, *21*, 1900664. [CrossRef]
9. Xiao, Y.; Zhang, Y.; Kaku, I.; Kang, R.; Pan, X. Electric vehicle routing problem: A systematic review and a new comprehensive model with nonlinear energy recharging and consumption. *Renew. Sustain. Energy Rev.* **2021**, *151*, 111567. [CrossRef]
10. Ren, L.; Kong, F.; Wang, X.; Song, Y.; Li, X.; Zhang, F.; Sun, N.; An, H.; Jiang, Z.; Wang, J. Triggering ambient polymer-based Li-O₂ battery via photo-electro-thermal synergy. *Nano Energy* **2022**, *98*, 107248. [CrossRef]
11. Ngo, N.-T. Early predicting cooling loads for energy-efficient design in office buildings by machine learning. *Energy Build.* **2019**, *182*, 264–273. [CrossRef]
12. Lin, L.; Chen, C.; Wei, B.; Li, H.; Shi, J.; Zhang, J.; Huang, N. Residential electricity load scenario prediction based on transferable flow generation model. *J. Electr. Eng. Technol.* **2022**, 1–11. [CrossRef]
13. Zhao, Y.; Foong, L.K. Predicting Electrical Power Output of Combined Cycle Power Plants Using a Novel Artificial Neural Network Optimized by Electrostatic Discharge Algorithm. *Measurement* **2022**, *198*, 111405. [CrossRef]
14. Zhao, Y.; Wang, Z. Subset simulation with adaptable intermediate failure probability for robust reliability analysis: An unsupervised learning-based approach. *Struct. Multidiscip. Optim.* **2022**, *65*, 172. [CrossRef]
15. Alduailij, M.A.; Petri, I.; Rana, O.; Alduailij, M.A.; Aldawood, A.S. Forecasting peak energy demand for smart buildings. *J. Supercomput.* **2021**, *77*, 6356–6380. [CrossRef]
16. Seyedzadeh, S.; Rahimian, F.P.; Oliver, S.; Rodriguez, S.; Glesk, I. Machine learning modelling for predicting non-domestic buildings energy performance: A model to support deep energy retrofit decision-making. *Appl. Energy* **2020**, *279*, 115908. [CrossRef]
17. Liu, Z.; Wu, D.; Liu, Y.; Han, Z.; Lun, L.; Gao, J.; Jin, G.; Cao, G. Accuracy analyses and model comparison of machine learning adopted in building energy consumption prediction. *Energy Explor. Exploit.* **2019**, *37*, 1426–1451. [CrossRef]
18. Qamber, I.S. Energy consumption prediction using Petri Nets-ANFIS development technique. *Arab. J. Basic Appl. Sci.* **2022**, *29*, 193–207. [CrossRef]
19. Bilgili, M.; Yildirim, A.; Ozbek, A.; Celebi, K.; Ekinici, F. Long short-term memory (LSTM) neural network and adaptive neuro-fuzzy inference system (ANFIS) approach in modeling renewable electricity generation forecasting. *Int. J. Green Energy* **2021**, *18*, 578–594. [CrossRef]
20. Baetens, J.; Van Eetvelde, G.; Lemmens, G.; Kayedpour, N.; De Koning, J.D.; Vandeveldel, L. Thermal performance evaluation of an induced draft evaporative cooling system through adaptive neuro-fuzzy interference system (anfis) model and mathematical model. *Energies* **2019**, *12*, 2544. [CrossRef]
21. Gao, W.; Moayedi, H.; Shahsavari, A. The feasibility of genetic programming and ANFIS in prediction energetic performance of a building integrated photovoltaic thermal (BIPVT) system. *Sol. Energy* **2019**, *183*, 293–305. [CrossRef]
22. Ekici, B.B.; Aksoy, U.T. Prediction of building energy needs in early stage of design by using ANFIS. *Expert Syst. Appl.* **2011**, *38*, 5352–5358.
23. Alam, S.M.; Ali, M.H. A new subtractive clustering based ANFIS system for residential load forecasting. In Proceedings of the 2020 IEEE Power & Energy Society Innovative Smart Grid Technologies Conference (ISGT), Washington, DC, USA, 17–20 February 2020; IEEE: Piscataway, NJ, USA, 2020; pp. 1–5.
24. Ahmad, M.W.; Mourshed, M.; Rezugui, Y. Trees vs Neurons: Comparison between random forest and ANN for high-resolution prediction of building energy consumption. *Energy Build.* **2017**, *147*, 77–89. [CrossRef]
25. Seyedzadeh, S.; Rahimian, F.P.; Rastogi, P.; Glesk, I. Tuning machine learning models for prediction of building energy loads. *Sustain. Cities Soc.* **2019**, *47*, 101484. [CrossRef]
26. Nilashi, M.; Dalvi-Esfahani, M.; Ibrahim, O.; Bagherifard, K.; Mardani, A.; Zakuan, N. A soft computing method for the prediction of energy performance of residential buildings. *Measurement* **2017**, *109*, 268–280. [CrossRef]
27. Zhao, Y.; Yan, Q.; Yang, Z.; Yu, X.; Jia, B. A novel artificial bee colony algorithm for structural damage detection. *Adv. Civ. Eng.* **2020**, *2020*, 3743089. [CrossRef]

28. Zhao, Y.; Moayedi, H.; Bahiraei, M.; Foong, L.K. Employing TLBO and SCE for optimal prediction of the compressive strength of concrete. *Smart Struct. Syst.* **2020**, *26*, 753–763.
29. Nguyen, H.; Mehrabi, M.; Kalantar, B.; Moayedi, H.; Abdullahi, M.a.M. Potential of hybrid evolutionary approaches for assessment of geo-hazard landslide susceptibility mapping. *Geomat. Nat. Hazards Risk* **2019**, *10*, 1667–1693. [[CrossRef](#)]
30. Kardani, N.; Bardhan, A.; Kim, D.; Samui, P.; Zhou, A. Modelling the energy performance of residential buildings using advanced computational frameworks based on RVM, GMDH, ANFIS-BBO and ANFIS-IPSO. *J. Build. Eng.* **2021**, *35*, 102105. [[CrossRef](#)]
31. Almutairi, K.; Algarni, S.; Alqahtani, T.; Moayedi, H.; Mosavi, A. A TLBO-Tuned Neural Processor for Predicting Heating Load in Residential Buildings. *Sustainability* **2022**, *14*, 5924. [[CrossRef](#)]
32. Lin, C.; Wang, J. Metaheuristic-designed systems for simultaneous simulation of thermal loads of building. *Smart Struct. Syst.* **2022**, *29*, 677–691.
33. Guo, Z.; Moayedi, H.; Foong, L.K.; Bahiraei, M. Optimal modification of heating, ventilation, and air conditioning system performances in residential buildings using the integration of metaheuristic optimization and neural computing. *Energy Build.* **2020**, *214*, 109866. [[CrossRef](#)]
34. Moayedi, H.; Mehrabi, M.; Mosallanezhad, M.; Rashid, A.S.A.; Pradhan, B. Modification of landslide susceptibility mapping using optimized PSO-ANN technique. *Eng. Comput.* **2019**, *35*, 967–984. [[CrossRef](#)]
35. Foong, L.K.; Zhao, Y.; Bai, C.; Xu, C. Efficient metaheuristic-retrofitted techniques for concrete slump simulation. *Smart Struct. Syst. Int. J.* **2021**, *27*, 745–759.
36. Mehrabi, M.; Pradhan, B.; Moayedi, H.; Alamri, A. Optimizing an adaptive neuro-fuzzy inference system for spatial prediction of landslide susceptibility using four state-of-the-art metaheuristic techniques. *Sensors* **2020**, *20*, 1723. [[CrossRef](#)] [[PubMed](#)]
37. Moayedi, H.; Mehrabi, M.; Kalantar, B.; Abdullahi Mu'azu, M.; Rashid, A.S.A.; Foong, L.K.; Nguyen, H. Novel hybrids of adaptive neuro-fuzzy inference system (ANFIS) with several metaheuristic algorithms for spatial susceptibility assessment of seismic-induced landslide. *Geomat. Nat. Hazards Risk* **2019**, *10*, 1879–1911. [[CrossRef](#)]
38. Adedeji, P.A.; Akinlabi, S.; Madushele, N.; Olatunji, O.O. Hybrid adaptive neuro-fuzzy inference system (ANFIS) for a multi-campus university energy consumption forecast. *Int. J. Ambient. Energy* **2022**, *43*, 1685–1694. [[CrossRef](#)]
39. Guleryuz, D. Determination of industrial energy demand in Turkey using MLR, ANFIS and PSO-ANFIS. *J. Artif. Intell. Syst.* **2021**, *3*, 16–34.
40. Panapakidis, I.P.; Dagoumas, A.S. Day-ahead natural gas demand forecasting based on the combination of wavelet transform and ANFIS/genetic algorithm/neural network model. *Energy* **2017**, *118*, 231–245. [[CrossRef](#)]
41. Yousri, D.; Babu, T.S.; Fathy, A. Recent methodology based Harris Hawks optimizer for designing load frequency control incorporated in multi-interconnected renewable energy plants. *Sustain. Energy Grids Netw.* **2020**, *22*, 100352. [[CrossRef](#)]
42. Sun, F.; Yu, J.; Zhao, A.; Zhou, M. Optimizing multi-chiller dispatch in HVAC system using equilibrium optimization algorithm. *Energy Rep.* **2021**, *7*, 5997–6013. [[CrossRef](#)]
43. Zayed, M.E.; Zhao, J.; Li, W.; Elsheikh, A.H.; Abd Elaziz, M. A hybrid adaptive neuro-fuzzy inference system integrated with equilibrium optimizer algorithm for predicting the energetic performance of solar dish collector. *Energy* **2021**, *235*, 121289. [[CrossRef](#)]
44. Wu, X.; Zheng, W.; Xia, X.; Lo, D. Data quality matters: A case study on data label correctness for security bug report prediction. *IEEE Trans. Softw. Eng.* **2021**, *48*, 2541–2556. [[CrossRef](#)]
45. Nguyen, M.-L.; Phung, T.; Ly, D.-H.; Truong, H.-L. Holistic Explainability Requirements for End-to-End Machine Learning in IoT Cloud Systems. In Proceedings of the 2021 IEEE 29th International Requirements Engineering Conference Workshops (REW), Notre Dame, IN, USA, 20–24 September 2021; IEEE: Piscataway, NJ, USA, 2021; pp. 188–194.
46. Chegari, B.; Tabaa, M.; Simeu, E.; Moutaouakkil, F.; Medromi, H. Multi-objective optimization of building energy performance and indoor thermal comfort by combining artificial neural networks and metaheuristic algorithms. *Energy Build.* **2021**, *239*, 110839. [[CrossRef](#)]
47. Jang, J.-S. ANFIS: Adaptive-network-based fuzzy inference system. *IEEE Trans. Syst. Man Cybern.* **1993**, *23*, 665–685. [[CrossRef](#)]
48. Ghenai, C.; Al-Mufti, O.A.A.; Al-Isawi, O.A.M.; Amirah, L.H.L.; Merabet, A. Short-term building electrical load forecasting using adaptive neuro-fuzzy inference system (ANFIS). *J. Build. Eng.* **2022**, *52*, 104323. [[CrossRef](#)]
49. Faramarzi, A.; Heidarinejad, M.; Stephens, B.; Mirjalili, S. Equilibrium optimizer: A novel optimization algorithm. *Knowl.-Based Syst.* **2020**, *191*, 105190. [[CrossRef](#)]
50. Zhao, Y.; Zhong, X.; Foong, L.K. Predicting the splitting tensile strength of concrete using an equilibrium optimization model. *Steel Compos. Struct. Int. J.* **2021**, *39*, 81–93.
51. Mirjalili, S.; Mirjalili, S.M.; Lewis, A. Grey wolf optimizer. *Adv. Eng. Softw.* **2014**, *69*, 46–61. [[CrossRef](#)]
52. Heidari, A.A.; Mirjalili, S.; Faris, H.; Aljarah, I.; Mafarja, M.; Chen, H. Harris hawks optimization: Algorithm and applications. *Future Gener. Comput. Syst.* **2019**, *97*, 849–872. [[CrossRef](#)]
53. Mirjalili, S.; Gandomi, A.H.; Mirjalili, S.Z.; Saremi, S.; Faris, H.; Mirjalili, S.M. Salp Swarm Algorithm: A bio-inspired optimizer for engineering design problems. *Adv. Eng. Softw.* **2017**, *114*, 163–191. [[CrossRef](#)]
54. Agwa, A.M. Equilibrium optimization algorithm for automatic generation control of interconnected power systems. *Prz. Elektrotechniczny* **2020**, *96*, 143–148. [[CrossRef](#)]
55. Yıldız, A.R.; Özkaya, H.; Yıldız, M.; Bureerat, S.; Yıldız, B.; Sait, S.M. The equilibrium optimization algorithm and the response surface-based metamodel for optimal structural design of vehicle components. *Mater. Test.* **2020**, *62*, 492–496.

56. Faris, H.; Aljarah, I.; Al-Betar, M.A.; Mirjalili, S. Grey wolf optimizer: A review of recent variants and applications. *Neural Comput. Appl.* **2018**, *30*, 413–435. [[CrossRef](#)]
57. Mirjalili, S.; Aljarah, I.; Mafarja, M.; Heidari, A.A.; Faris, H. Grey wolf optimizer: Theory, literature review, and application in computational fluid dynamics problems. In *Nature-Inspired Optimizers*; Springer: Berlin/Heidelberg, Germany, 2020; pp. 87–105.
58. Alabool, H.M.; Alarabiat, D.; Abualigah, L.; Heidari, A.A. Harris hawks optimization: A comprehensive review of recent variants and applications. *Neural Comput. Appl.* **2021**, *33*, 8939–8980. [[CrossRef](#)]
59. Qu, C.; He, W.; Peng, X.; Peng, X. Harris hawks optimization with information exchange. *Appl. Math. Model.* **2020**, *84*, 52–75. [[CrossRef](#)]
60. Abualigah, L.; Shehab, M.; Alshinwan, M.; Alabool, H. Salp swarm algorithm: A comprehensive survey. *Neural Comput. Appl.* **2020**, *32*, 11195–11215. [[CrossRef](#)]
61. Faris, H.; Mirjalili, S.; Aljarah, I.; Mafarja, M.; Heidari, A.A. Salp swarm algorithm: Theory, literature review, and application in extreme learning machines. In *Nature-Inspired Optimizers*; Springer: Berlin/Heidelberg, Germany, 2020; pp. 185–199.
62. Zhao, Y.; Hu, H.; Song, C.; Wang, Z. Predicting Compressive Strength of Manufactured-Sand Concrete Using Conventional and Metaheuristic-Tuned Artificial Neural Network: Abbreviated Title: Various ANNs for Modeling Concrete Strength. *Measurement* **2022**, *194*, 110993. [[CrossRef](#)]
63. Mehrabi, M. Landslide susceptibility zonation using statistical and machine learning approaches in Northern Lecco, Italy. *Nat. Hazards* **2021**, *111*, 901–937. [[CrossRef](#)]
64. Moayedi, H.; Raftari, M.; Sharifi, A.; Jusoh, W.A.W.; Rashid, A.S.A. Optimization of ANFIS with GA and PSO estimating α ratio in driven piles. *Eng. Comput.* **2020**, *36*, 227–238. [[CrossRef](#)]
65. Wu, D.; Foong, L.K.; Lyu, Z. Two neural-metaheuristic techniques based on vortex search and backtracking search algorithms for predicting the heating load of residential buildings. *Eng. Comput.* **2020**, *38*, 647–660. [[CrossRef](#)]
66. Moayedi, H.; Mosavi, A. Suggesting a stochastic fractal search paradigm in combination with artificial neural network for early prediction of cooling load in residential buildings. *Energies* **2021**, *14*, 1649. [[CrossRef](#)]
67. Mu'azu, M.A. Enhancing Slope Stability Prediction Using Fuzzy and Neural Frameworks Optimized by Metaheuristic Science. *Math. Geosci.* **2022**, 1–23. [[CrossRef](#)]
68. Moayedi, H.; Mehrabi, M.; Bui, D.T.; Pradhan, B.; Foong, L.K. Fuzzy-metaheuristic ensembles for spatial assessment of forest fire susceptibility. *J. Environ. Manag.* **2020**, *260*, 109867. [[CrossRef](#)] [[PubMed](#)]
69. Mehrabi, M.; Moayedi, H. Landslide susceptibility mapping using artificial neural network tuned by metaheuristic algorithms. *Environ. Earth Sci.* **2021**, *80*, 804. [[CrossRef](#)]
70. Taylor, K.E. Summarizing multiple aspects of model performance in a single diagram. *J. Geophys. Res. Atmos.* **2001**, *106*, 7183–7192. [[CrossRef](#)]
71. Wu, Y.-H.; Shen, H. Grey-related least squares support vector machine optimization model and its application in predicting natural gas consumption demand. *J. Comput. Appl. Math.* **2018**, *338*, 212–220. [[CrossRef](#)]
72. Al-bayaty, H.; Mohammed, T.; Ghareeb, A.; Wang, W. City scale energy demand forecasting using machine learning based models: A comparative study. In Proceedings of the Second International Conference on Data Science, E-Learning and Information Systems, Dubai, United Arab Emirates, 2–4 December 2019; pp. 1–9.
73. Moayedi, H.; Osouli, A.; Nguyen, H.; Rashid, A.S.A. A novel Harris hawks' optimization and k-fold cross-validation predicting slope stability. *Eng. Comput.* **2021**, *37*, 369–379. [[CrossRef](#)]
74. Zheng, Y.; Jin, H.; Jiang, C.; Moradi, Z.; Khadimallah, M.A.; Moayedi, H. Analyzing behavior of circular concrete-filled steel tube column using improved fuzzy models. *Steel Compos. Struct.* **2022**, *43*, 625–637.